Author's Accepted Manuscript

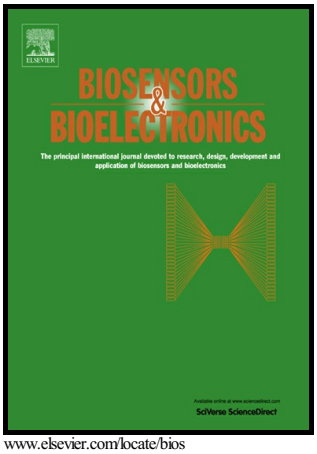

www.elsevier.com/locate/bios

Nickel nanoclusters as a novel emitter for molecularly imprinted electrochemiluminescence based sensor toward nanomolar detection of creatinine

Bahareh Babamiri, Abdollah Salimi, Rahman Hallaj

PII: S0956-5663(18)30110-6
DOI: https://doi.org/10.1016/j.bios.2018.02.022
Reference: BIOS10284

To appear in: *Biosensors and Bioelectronic*

Received date: 6 December 2017
Revised date: 24 January 2018
Accepted date: 7 February 2018

Cite this article as: Bahareh Babamiri, Abdollah Salimi and Rahman Hallaj, Nickel nanoclusters as a novel emitter for molecularly imprinted electrochemiluminescence based sensor toward nanomolar detection of creatinine, *Biosensors and Bioelectronic,* https://doi.org/10.1016/j.bios.2018.02.022

Nickel nanoclusters as a novel emitter for molecularly imprinted electrochemiluminescence based sensor toward nanomolar detection of creatinine

Bahareh Babamiri,[a] Abdollah Salimi,[a,b*] Rahman Hallaj[a,b*]

[a]Department of Chemistry, University of Kurdistan, 66177-15175, Sanandaj, Iran

[b]Research Center for Nanotechnology, University of Kurdistan, 66177-15175, Sanandaj, Iran

[a]Department of Chemistry, University of Kurdistan, 66177-15175, Sanandaj, Iran

[b]Research Center for Nanotechnology, University of Kurdistan, 66177-15175, Sanandaj, Iran

Corresponding authors: Tel.: +98 8733624001; fax: +98 87336624008.

E-mail addresses: absalimi@uok.ac.ir, absalimi@yahoo.com (A.Salimi), Rhallaj@uok.ac.ir, (R. Hallaj)

ABSTRACT

In this study nickel nanoclusters (NiNCs), was promised as novel and economic electrochemiluminescence (ECL) emitter for highly sensitive and selective determination of creatinine in the presence of molecularly imprinted polymer (MIP). The uniform magnetic graphene oxide (GO-Fe_3O_4) MIP film was established on the surface of ITO electrode and Ni NCs-embedded in MIP, showed a strong anodic ECL emission using tri-n-propylamine (TPrA) as coreactant. During the ECL process, TPrA was oxidized, and Ni NCs got the energy to generate excited state Ni NCs* for light emission. When the imprinted cavities were occupied by creatinine, the ECL emission of Ni NCs on the MIP-modified electrode surface was efficiently quenched. Under optimal conditions, the proposed sensor demonstrated ultrasensitive and accurate analytical performance toward creatinine detection with a linear range from 5 nM to 1 mM and detection limit of 0.5 nM (S/N=3). The biosensor showed good specificity for creatinine determination compared to other compounds that having the chemical structure analogue or close to the template creatinine, when the concentration ratio of interference to creatinine was more than 100 times. Furthermore, the biosensor was successfully applied to determination of creatinine in human serum and urine samples with satisfactory results. So, this assay for creatinine detection possesses high sensitivity, good selectivity, excellent reproducibility and stability. We expect the combination of molecular imprinting system with ECL assay in the presence of Ni NCs as a new type of superior luminophore candidate can be developed for design of ultrasensitive sensors, biosensors and other measuring devices.

Keywords: Molecularly imprinted polymer, Electrochemiluminescence sensor, Ni nanoclusters, Creatinine.

1. Introduction

Creatinine (Cre) is the final product of the metabolism of creatine in mammals that removed from the body by kidneys through glomerular filtration at a relatively constant rate (Chen et al., 2006). Since the concentration of creatinine is less affected by the dietary changes, therefore the accurate and sensitive detection of low level quantities of creatinine in blood and urine is a fairly reliable indicator in the clinical evaluation of renal function, the severity of kidney damage, muscular disorders and thyroid malfunction (Yamato et al., 1995). Clinical analysis of creatinine is routinely carried out using the conventional techniques, such as colorimetric Jaffe reaction and enzymatical reaction (Slot 1965). However, Jaffe's method suffers from poor selectivity of picric acid toward numerous metabolites containing carbonyl group found in biological samples, such as proteins, glucose, bilirubin, and ascorbic acid (Weber and Van Zanten 1991). Selectivity can be enhanced by the use of enzymatic detection methods based on a series of sequential enzyme-mediated steps that result in the formation of hydrogen peroxide (Fossati et al., 1983). Although the introduction of enzymes has improved specificity, but enzymes suffer from instability, high cost and complex procedures for the immobilization (Lad et al., 2008). Therefore, the development of sensitive, selective, facile, rapid and low cost analytical techniques for the detection of creatinine have attracted great attention.

In recent years, molecularly imprinted polymers (MIPs) have been used to developing new generation of chemical/biological sensors due to their superiorities such as high adsorption capacity, high specific recognition of target molecules, desirable physical and chemical stability, excellent reusability, low cost and easy preparation offers (Chen et al., 2011; Wulff 2013). However, MIPs prepared by the conventional technique have few disadvantages such as low-affinity binding, incomplete template removal, high diffusion barrier and slow mass transfer,

lack of conductivity and electrocatalytical activity which leads to the limitation of these MIPs (Alexander et al., 2017). Imprinting of target molecules on the surface of nanostructure such as silica beads (Wang et al., 2014), quantum dot (Huy et al., 2014), carbon nanotubes (Zhao et al., 2014), Fe_3O_4 nanoparticles (Gao et al., 2014) and graphene (Chen et al., 2016) can be an effective method to eliminate these constraints. Among different kinds of nanostructures, graphene oxide (GO) with an extremely large specific surface area and magnetic NPs with strong superparamagnetic properties are excellent candidates as a support material for preparing surface MIPs to improve accessibility of the recognition sites, binding capacity, and binding kinetics (Ning et al., 2014). Hence, with combination the advantages of surface imprinted polymer and GO-Fe_3O_4 composites, efficient adsorbent materials with high selectivity, specific recognition ability, large adsorption capacity, easy manipulation and magnetic properties can be fabricated (Luo et al., 2016). During recent years, molecularly imprinted polymer based electrochemical (Xie et al., 2010) and chemiluminescence (Lin and Yamada, 2000) sensors have been developed for the signal detection in MIP sensors. However, these methods can hardly be applied for ultra-trace analysis because of their insufficient sensitivities. Therefore, the development of a novel strategy for the highly sensitive determination of the ultra-trace amounts of different targets by using the MIP sensors is an obvious demand.

Electrochemiluminescence (ECL) assay developed as new opportunities for analytical methodology, due to its high sensitivity, low background signal, excellent controllability, rapidness and simple sample pretreatment procedures (Babamiri et al.,2017, Babamiri et al., 2018 a; Richter 2004; Miao 2008). Therefore, with the combining the numerous superiorities of both MIP and ECL assays, the MIP-ECL sensor offered the advantages of high detection sensitivity and selectivity, wide dynamic concentration response range, reusability, chemical and

mechanical stability and high precision (Li et al., 2013; Yang et al., 2016). Recently, different quantum dots were used as emitters in ECL, while the inherent toxicity of the QDs due to the presence of heavy metals such as Cd^{2+} and Pb^{2+} in their structure led to restrictions in the application of bioassay (Wu, et al., 2017; Huy et al., 2014). Thus, to reduce environmental pollution, development of a novel low-toxicity or nontoxic ECL species for bioanalysis is necessary. Lately, noble metal nanoclusters (MNCs) (with the size smaller than 2 nm) because of their unique outstanding electrical conductivity and excellent biocompatibility properties have attracted great attention in fundamental and practical application of fluorescent biolabeling, chemical sensing and biosensor assays (Xiao et al., 2015; Sementa et al., 2015). Au nanoclusters (Au NCs) and silver nanoclusters (Ag NCs) due to specific optical, electronic, and chemical properties have been used as electrochemiluminescence labels for chemical sensing and bio imaging (Fang et al., 2011; Liu et al., 2013). Due to the high consumption of gold and silver, significant efforts have been done to find a low-cost candidate with high-efficiency optical properties as ECL emitters.

Herein, in continues to previous studies for development of ECL assay for analysis of various analytes (Babamiri et al., 2018 b,c) stable and water-soluble Ni nanoclusters (Ni NCs) capped with a model protein, bovine serum albumin (BSA) as a novel photoluminescent nanomaterial is prepared. Due to excellent photoluminescence property of Ni NCs, for the first time the fluorescence emission and the anodic ECL emission of Ni nanoclusters in aqueous solution at the presence of tri-propyl amine (TPA) as coreactant agent was investigated. The Ni nanoclusters (Ni NCs) was used as luminescent signal source, for ECL detection of creatinine in the presence of creatinine molecularly imprinted polymer formed by sol-gel method using creatinine as template and tetraethyl orthosilicate (TEOS) as cross-linker on the surface of ITO electrode and

aluminum chloride was introduced to MIP for increase the binding affinity of the creatinine into cavities. In this work, a composite material (MIP@GO-Fe_3O_4) based on molecular imprinted polymer (MIP), superparamagnetic Fe_3O_4 particles and graphene oxide (GO) was used for creatinine determination, because it combined all of the advantages from MIP, superparamagnetic Fe_3O_4 and GO. The ITO electrode modified with MIP film containing Ni NCs showed a strong and stable ECL with the co-reactant TPrA. In the presence of creatinine, the ECL of Ni NCs was efficiently quenched and the responses of the proposed sensing decreased with the increasing of creatinine concentration. The proposed sensor can be applied for subnanomolar detection of creatinine in serum and urine samples.

Experimental

2.1. Chemicals and Apparatus

All chemicals were analytical grade were purchased from Sigma-Aldrich. The applied instruments for electrochemical measurements, microscopic imaging and nanomaterial characterization were reported in supporting information file(SI).

2.2. Synthesis of nickel nanoclusters and magnetic graphene oxide (GO-Fe_3O_4)

Ni NCs@BSA was directly synthesized in aqueous solution using the hydrothermal method according to previously reported process (Zhao et al., 2016), with a minor modification and details is reported in SI. Furthermore, the details for GO-Fe_3O_4 synthesis process reported in SI.

2.3.Fabrication of molecular imprinted polymer modified electrode

The fabrication process of the ECL assay is illustrated in scheme 1. Firstly, 100 mg of creatinine and 300 mg of $AlCl_3.6H_2O$ were added into a mixture containing 2 mL TEOS, 1 mL HCl solution (1M) and 4 mL deionized water. Then the clean ITO electrode was immersed in the solution, while stirred for 2 h at room temperature. In the following, 0.4 g GO-Fe_3O_4 and 3.16

mL Ni NCs were added to the above solution, and the reaction was allowed under stirring to continue for 24 h. The MIPs were fabricated on the surface of ITO electrode via a typical sol-gel polymerization. It should be noted that the ITO electrode is participates in the polymerization process through the surface hydroxyl groups. The modified ITO electrode was washed with ultrapure water and immersed in anhydrous ethanol solution to remove creatinine template until no creatinine could be detected in the washing solvent using UV spectrometry technique. For comparison, the non-imprinted polymers (NIP) was prepared under the same conditions without adding of template molecules (creatinine).

2.4. ECL detection

For creatinine detection, MIP modified electrode was immersed into the standard solution containing different concentrations of creatinine for 15 min. The electrode was washed with water to remove the unbound creatinine. Then, the modified electrode was immersed in 0.1 M PBS (pH 7.4) containing 0.01 M TPrA under applied potential cycling from 0.0 to 1.5 V with a scan rate of 100 mV s^{-1}, while during detection process, the voltage of the photomultiplier tube was set at 800 V. The ECL signals related to the creatinine concentrations were measured by placing a band-pass filter of 330 nm before the PMT window. For the PL detection, 20 mL of MIPs suspensions (0.05 mg mL^{-1}) and the standard solution containing different concentrations of creatinine were mixed and stirred under room temperature for 15 min. Then, 200 μL above mixture were injected into the cuvette. The fluorescence intensity was recorded at 375 nm with the excitation of 230 nm and both the excitation and emission slits were set as 5 nm.

3. Results and discussions

3.1. Morphology and structure characterization of Ni NCs

The size distribution and morphology of the as-prepared Ni NCs were characterized by HRTEM (Figure 1A). As seen in Figure 1A, the prepared Ni NCs were spherical and monodisperse, with uniform distribution. TEM analysis showed that Ni NCs were mainly distributed in the range 2-4.5 nm with the mean particle size of approximately 2.7 nm (the inset of Figure 1A). In accordance to the TEM image, based on the AFM images the average size of Ni NCs was estimated 2-3 nm (Figure 1B, C). To characterize the optical properties of Ni NCs, the UV-vis absorption and fluorescence emission spectra at different excitation wavelengths were recorded. The UV-vis spectrum showed that the Ni NCs exhibit a considerable UV-vis absorption band centered at approximately 250 nm (Figure 1D). Furthermore, the excitation-dependent fluorescence spectra of Ni NCs in the range of 210-340 nm is shown in Fig.1D. It can be seen that, the PL emission wavelength gradually red-shift with varying excitation wavelengths and reached to the maximum value at 350 nm, then the PL intensity gradually decreased. The as-synthesized Ni NCs solution was bright orange under visible light, but exhibits bright green luminescence under UV lamp irradiation with a wavelength of 365 nm (the inset in Figure 1D). As shown in Figure 1E, the ECL spectrum of the Ni NCs demonstrated a maximum wavelength at 375 nm with a slight red-shift (350 to 375 nm) in a comparison with the PL spectrum which indicated radical ion and triplet-triplet annihilation leading to some excimer formation. The FTIR spectroscopy was utilized to investigate the surface state and chemical structure of the Ni NCs by the comparison of monomeric BSA and BSA-protected Ni NCs (Figure 1F). In the case of monomeric BSA, the broad peak at 3310 cm^{-1} was attributed to stretching of the amino group (NH_2), and the peak at 1170 cm^{-1} was assigned to the C-N bending vibration. The absorption bands at 2959 and 2875 cm^{-1} correspond to the asymmetric and symmetric vibrations of CH_2, respectively. The characteristic amide I band in 1600-1700 cm^{-1} was attributed to the stretching

vibration of C=O. Also, the amide (II) peak at 1550 cm^{-1} was assigned to the typical vibrational profiles of BSA (C-N stretching and N-H bending). The peaks at about 1120 and 1400 cm^{-1} were attributed to C=O deformation and C-O stretching, respectively. The obtained results indicating the presence of the characteristic functional groups of carboxyl (COOH) and amino (NH_2) in the BSA structure. When the BSA was used as a protecting agent for the Ni NCs formation, the characteristic peaks of Ni NCs from the corresponding FTIR spectrum (curve b) showed a little red-shift in comparison to characteristic peaks of BSA (Zhao et al., 2016). The reason indicates that Ni (II) first coordinated with the NH_2 and SH groups of BSA and then reduced to Ni (0) equipped with BSA as the protecting ligand. The crystal structure of the prepared Ni NCs was characterized by XRD. According to the XRD of the as-prepared Ni NCs (Figure 1G), sharp diffraction peaks at 44.5, 51.8 and 76.42 degrees of 2θ, corresponds to (111), (200) and (220) faces of a Ni crystal were observed, which demonstrate the formation of metallic Ni. The obtained results were in good agreement with the reference file (JCPDS file 65-0380). The XRD line broadenings for the samples prepared, which suggested a smaller crystallite size in these samples with no impurity peaks. Moreover, X-ray photoelectron spectroscopy (XPS) survey spectra of the as-prepared Ni NCs confirmed that the Ni NCs were made up of all the expected elements including C, O, N, S, Na, and Ni (Figure 1H). Furthermore, as illustrated in Figure 1I, two characteristic peaks were observed at 855.28 and 871.68 eV, which were attributed to $2p_{3/2}$ and $2p_{1/2}$ features of metallic Ni (Perkin et al., 1979). Moreover, shakeup was noted at 861.48 and 880.28 eV, indicating the minimal presence of Ni (II) in the as-prepared Ni NCs. In addition, SEM images of the MIPs illustrated that the MIPs film was uniform and showed high density distribution (Figure 2 A, B). In comparison, the SEM image of NIPs showed relatively sparse and unevenly distribution (Figure 2 C, D). Also, the morphological structures and the magnetic

property of GO-Fe_3O_4 and MIP-GO-Fe_3O_4 were examined by SEM and alternative gradient force magnetometer (AGFM). (reported in SI as Fig. S1 and S2). The obtained results confirmed that Fe_3O_4@GO and MIP@Fe_3O_4@GO were prepared successively. Fig. S3 showed the ECL emission of MIP-modified electrode with and without GO-Fe_3O_4 respectively, after removal of creatinine from polymer and after incubating in creatinine solution for 15 min. Without GO-Fe_3O_4, the MIP-modified electrode illustrated very low ECL signal, which proved GO-Fe_3O_4 accelerate the electron transfer and the conductivity and increase the specific surface area. The obtained result confirmed that the MIPs provides a large surface area for the adsorption of the target analyte at the surface of modified electrode.

3.2. Effects of coreactants toward Ni NCs

To investigate the effect of coreactant toward the ECL response of Ni NCs, the ECL spectra of Ni NCs in the presence of three different anodic coreactants (TPA, HZ and H_2O_2) were recorded. Firstly, the bare ITO electrode was immersed in 0.1 M PBS (pH 7.4) containing 10 μg mL^{-1} Ni NCs and potential scanned from 0.0 to 1.5 V with a scan rate of 100 mV s^{-1}. In the following, the above-mentioned three coreactants were added into the testing buffer, respectively. It can be seen that, the ECL responses of Ni NCs with HZ and H_2O_2 as coreactant increased weakly compared to the ECL response of the pure Ni NCs (Fig. S4 A, B), while in the presence of TPrA the ECL response was significantly increased (Fig. S4 C). So, TPrA can be used as an efficient coreactant to amplify the ECL emission of Ni NCs.

3.3. ECL mechanism response of the Ni NCs

The anodic ECL properties of Ni NCs at ITO electrode were studied. With TPrA as a co-reactant the as-prepared QDs showed a strong ECL emission peak at +1.2 V with an onset potential of +0.9 V. The possible emission ECL mechanism with TPrA as a co-reactant are

described which is the same with the ECL emission of the reported semiconductors (Zhang et al., 2016) with the following equations (1) - (6):

$$TPrA - e^- \rightarrow TPrA^{\bullet +} \quad (1)$$

$$Ni\ NCs + TPrA^{\bullet +} \rightarrow Ni\ NCs^{+} + TPrA \quad (2)$$

$$TPrA^{\bullet +} \rightarrow TPrA^{\bullet} + H^{+} \quad (3)$$

$$Ni\ NCs + TPrA^{\bullet} \rightarrow Ni\ NCs^{-} + Pr_2N^{+}CH_2\text{-}CH_3 \quad (4)$$

$$Ni\ NCs^{+} + Ni\ NCs^{-} \rightarrow Ni\ NCs^{*} + Ni\ NCs \quad (5)$$

$$Ni\ NCs^{*} \rightarrow Ni\ NCs + h\nu \quad (6)$$

3.4. Photoluminescence and ECL quenching of Ni NCs by creatinine

The quenching mechanism of creatinine toward photoluminescence of Ni NCs was evaluated. As shown in Figure 3A, the fluorescence intensity of Ni NCs@MIPs decreased gradually with increasing the concentration of creatinine from 1 μM to 0.1 M and a linear relationship between F_0-F and logarithmic value of creatinine concentration with the linear regression equation F_0-F = 152.13 lg *c* +967.86 and R^2 of 0.991 was obtained (Fig.3B), while the calculated detection limit of the assay was 0.1 μM (S/N=3). We suggest a charge transfer from Ni NCs to creatinine species is responsible for the fluorescence quenching of the Ni NCs. Generally, creatinine may quench the fluorescence of the Ni NCs with the band gap close to the absorption band edge of creatinine through a charge-transfer process that this mechanism has also been reported by (Tu et al., 2008; Wang et al., 2009). The UV absorption band of creatinine (225 and 245 nm) is close to the band gap of the Ni NCs as revealed by the absorption spectra of Ni NCs (Figure 1D) and creatinine (Figure 3C, b). The charges at the conductive band of the nanocrystals can directly transfer to the LUMO of the UV band of the creatinine. We can exclude energy transfer as a

possible mechanism for fluorescence quenching because there is low spectral overlap between the absorption spectra of creatinine and the emission spectrum of the Ni NCs (Figure 3C). Furthermore, as illustrated in Fig.3D creatinine quenched the ECL signal of Ni NCs. In this process, when the concentrations of creatinine increased, more cavities of MIP were blocked by the template molecule of creatinine. With blocking the cavities with creatinine, the touch of Ni NCs with TPrA was difficult and the ECL intensity decreased.

3.5. Monitoring of the biosensor fabrication by EIS

To investigate the changes of electrode behavior after each assembly step, electrochemical impedance spectroscopy (EIS) was performed and the obtained results are shown in Figure S5. The bare ITO electrode revealed a small semicircle profile (curve a). When the surface of ITO electrode was coated by imprinted polymer film, the resistance obviously increased (curve b). In the following, with elution the creatinine from the imprinted polymer, cavities act as the channels for electron transfer and decreasing in resistance was observed (curve c). Finally, with incubating the imprinted polymer by the template molecule, creatinine rebound with imprinted film coated on the surface of ITO electrode, the resistance increased again because the channels of electron transfer would be blocked (curve d). The EIS results confirmed that the ECL biosensor was successfully fabricated.

3.6. Analytical performance of the MIP-ECL sensor

Prior to creatinine measuring the parameters which affected to the ECL signal response was optimized. First investigate the effect of rebinding time of creatinine, the ECL measurements in the presence defined concentration of creatinine were performed in the range 10 to 60 min. As illustrated in Fig. S6, with increasing rebinding time, the ECL signal gradually decreased and reached the minimum value at 15 min. Therefore, 15 min was selected as the optimal incubation

time for the subsequent experiments. To synthesize stable Ni NCs with strong ECL emission, the amount of BSA as the protecting ligands should be sufficient in the synthetic process. As can be seen, a strongest ECL response was obtained when the concentration of BSA was 15.0 mg mL^{-1} in Ni NCs synthesis (Fig. S7). So, concentration of 15.0 mg mL^{-1} was chosen as the optimum amount of BSA in this experiment. Also, the effect of pH on ECL response were investigated by recording of ECL signal the pH values (6.0, 6.5, 7.0, 7.4, 8.0, 8.5, and 9.0). As illustrated in Fig. S8 The ECL intensity first increased with an increase in the pH, reached a maximum value at pH 7.4, and then decreased gradually. So, pH 7.40 was selected as the optimal pH value in the following detection process.

Under the optimized experimental conditions, the ECL response of the MIP sensor in the presence of various concentrations of creatinine was recorded. As shown in Figure 4A, with increasing concentration of creatinine, ECL intensity gradually decreased within the range from 5 nM to 1 mM and a linear relationship between ΔI_{ECL} ($\Delta I=I_0-I$) and logarithmic value of creatinine concentration with the linear regression equation of ΔI= 133.15 lg (c/μM) +396.17 and correlation coefficient of 0.9926 was obtained, while estimated detection limit was 0.5 nM at a signal-to-noise ratio of 3. Compared to all previously reported methods for creatinine detection (Table 1A), the MIP-ECL sensor based on the novel Ni NCs/TPrA ECL system showed a higher sensitivity, a wider response range and lower limit of detection.

3.7. Specificity, reproducibility and stability of the sensor for creatinine detection

To investigate the selectivity of the proposed system, the response of the MIP-based ECL sensor toward creatinine at concentration of 0.01 mM compared to 1 mM of creatine, N-hydroxysuccinimide (NHS) and 1-Methyl-2-pyrrolidinone (NMP) (compounds that having the

chemical structure analogue or close to the template creatinine) was investigated by measuring the ECL quenching values under the optimum conditions. As illustrated in Figure 4C, the MIP sensor shows significant ECL quenching in response to creatinine, but in the presence of other analogues, the ECL quenching of the sensor was quite low. Furthermore, the ECL quenching obtained from the mixture containing the above three interference and creatinine was almost the same as the value obtained from pure creatinine. Obviously, these results demonstrated that the introduced imprinted molecular recognition sites can selectively bind the template creatinine and then produce significant ECL quenching. Therefore, the MIP-based ECL sensor can be applied for selective detection of creatinine. Also, in comparison with the MIP-ECL sensor, the non MIP-ECL sensor showed a little ECL quenching (Figure 4D). The obtained results suggested that the NIPs could not effectively bind creatinine. To investigate the effect of foreign coexisting substances on the analysis of creatinine further interference experiments were recorded in the presence of creatinine together with other co-existing ions (Na^+, K^+, Ca^{2+}, Mg^{2+}, Cl^-, NO_3^-). It can be seen that there is no obvious effect on the determination of creatinine (Figure 4E). The reproducibility of the proposed sensor was evaluated by measuring the ECL intensity of 0.1 mM creatinine using five different sensors that were prepared in similar conditions. The relative standard deviations (RSD) of the five independent assays was 3.41 %, indicating a desirable accuracy and reproducibility of the ECL assay. To investigate the long-time stability of the MIP-ECL sensor for the determination of creatinine, ECL intensity were recorded over a period of 6 weeks, the sensor was stored in 4 °C when not in use. It was found that after a storage period of 6 weeks, over 90% of the initial response remained. The obtained results indicated that the proposed MIP-ECL sensor has acceptable storage stability and it can be used for a sufficiently long time. Additionally, the ECL intensities of the MIP sensor was recorded under continuous

potential scanning for 10 cycles. As shown in Figure 4F, the relative standard deviation (RSD) was less than 2.1%, indicating an acceptable stability of the proposed sensor for ECL detection.

3.8. Analysis of creatinine in serum and urine samples

For assessing the feasibility and potential applicability of the proposed assay, the MIP-ECL sensor was employed to determine creatinine in serum and urine samples with the standard addition method. The human serum and urine samples were obtained from the Verdi Clinical laboratory and Tawhid Hospital in Sanandaj-Iran. Because the concentration of serum and urine creatinine was nearly 20 μM and 20 mM respectively, 10-fold diluted serum and 100-fold diluted urine was applied in the following experiment and the obtained results were compared with clinical laboratory analysis (colorimetric assay) as the standard method. Furthermore, the serum and urine samples were spiked with different concentrations of creatinine and analyzed by the proposed sensor. As shown in Table 1B, the recoveries were obtained with a satisfied result from 90.02-99.68% with RSD of 1.81 to 3.53%, which confirmed that the proposed sensor was applicable for creatinine detection in biological samples.

3. Conclusions

In summary, Ni NCs was used as emitter for development of novel MIP-ECL sensor for selective detection of creatinine. The anodic ECL of the Ni NCs demonstrated with the employment of TPrA as a desired coreactant, using ITO electrode modified with a MIP and GO-Fe_3O_4 composites as platform. Due to the high adsorption capacity of GO-Fe_3O_4 composites for immobilized template per unit surface area the ECL signal and recognition capacity of the sensor for creatinine detection was improved. Using this excellent probe, a signal-off ECL sensor for creatinine detection with the detection limit down to 5×10^{-10} M and concentration range 6 orders of magnitude was developed. Furthermore, combining MIP with ECL improved the

selectivity of the ECL sensor and overcome the interference to the template molecule. the MIP-ECL sensor have demonstrated outstanding features such as high sensitivity and selectivity, wide dynamic range, high precision and the good stability. The obtained results demonstrated that Ni NCs with low cost provided can be alternative candidates for expensive and toxic ECL emitters. Finally, Ni NCs as novel emitter can be a promising candidate to fabricate of various MIP-ECL sensors or biosensors with improved sensitivity and sensitivity.

Acknowledgments

This research was supported by the Iranian Nanotechnology Initiative and the Research Office of the University of Kurdistan.

References

Alexander, S., Baraneedharan, P., Balasubrahmanyan, S., Ramaprabhu, S., 2017. Eur. Polym. J. 86, 106-116.

Babamiri, B., Hallaj, R., Salimi, A., 2018a. Biosens. Bioelectron. 99, 353-360.

Babamiri, B., Hallaj, R., Salimi, A., 2018b. Sens. Actuators B 254, 551-560.

Babamiri, B., Salimi, A., Hallaj, R., 2018c. Biosens. Bioelectron, 102, 328-335.

Babamiri, B., Hallaj, R., Salimi, A., Akhtari, K., 2017. Microchim. Acta 184, 3613-3623.

Chen, F., Zhao, W., Zhang, J., Kong, J., 2016. Phys. Chem. Chem. Phys. 18, 718-725.

Chen, J., Kumar, A. S., Chung, H., Chien, S., Kuo, M., Zen, J., 2006. Sens. Actuators B 115, 473-480.

Chen, L., Xu, S., Li, J., 2011. Chem. Soc. Rev. 40, 2922-2942.

Debus, B., Kirsanov, D., Yaroshenko, I., Sidorova, A., Piven, A., Legin, A., 2015. Anal. Chim. Acta 895, 71-79.

Fang, Y., Song, J., Li, J., Wang, Y. W., Yang, H. H., Sun, J. J., Chen, G. N., 2011. Chem. Commun. 47, 2369-2371.

Fossati, P., Prencipe, L., Bertl, G., 1983. Clin. Chem. 29, 1494-1496.

Gao, R., Mu, Y., Yi Hao, Y., Zhang, L., Zhang, J., Tang, Y., 2014. J. Mater. Chem. B 2, 1733-1741.

Handbook of X-ray Photoelectron Spectroscopy, vol. 55, Physical Electronic Division, Perkin-Elmer, 1979, p. 344.

Hanif, S., John, P., Gao, W., Saqib, M., Qi, L., Xu, G., 2016. Biosens. Bioelectron. 75, 347-351.

He, Y., Zhang, X., Yu, H., 2015. Microchim. Acta 182, 2037-2043.

Huy, B., Seo, M., Zhang, X., Lee, Y., 2014. Biosens. Bioelectron. 57, 310-316.

Khadro, B., Sanglar, C., Bonhomme, A., Errachid, A., 2010. Procedia Eng. 5, 371-374.

Lad, U., Khokhar, S., Kale, G. M., 2008. Anal. Chem. 80, 7910-7917.

Li, H., Xie, C., Fu, X., 2013. Sens. Actuators B 181, 858- 866.

Lin, J., Yamada, M., 2000. Anal. Chem. 72, 1148-1155.

Liu, T., Zhang, L., Song, H., Wang, Z., Lv, Y., 2013. Luminescence 28, 530-535.

Luo, J., Gao, Y., Tan, K., Wei, W., Liu, X., 2016. ACS Sustainable Chem. Eng. 4, 3316-3326.

Luo, J., Jiang, S., Zhang, H., Jiang, J., Liu, X., 2012. Anal. Chim. Acta 709, 47-53.

Miao, W., 2008. Chem. Rev.108, 2506-2553.

Ning, F., Peng, H., Chen, L., Xiong, H., Li, J., 2014. *J. Agric. Food Chem.* 62, 7436-7443.

Richter, M. M., 2004. Chem. Rev. 104, 3003-3036.

Sementa, L., Barcaro, G., Dass, A., Stener, M., Fortunelli, A., 2015. Chem. Commun. 51**,** 7935-7938.

Slot, C., 1965. Scand. J. Clin. Lab. Invest. 17, 381-387.

Subrahmanyam, S., Piletsky, S. A., Piletska, E. V., Chen, B., Karim, K., Turner.A. P. F., 2001. Biosens. Bioelectron. 16, 631-637.

Tu, R.Y., Liu, B. H., Wang, Z. Y., Gao, D. M., Wang, F., Fang, Q. L., Zhang, Z. P., 2008. Anal. Chem. 80, 3458-3465.

Wang, H. F., He, Y., Ji, T. R., Yan, X. P., 2009. Anal. Chem. 81, 1615-1621.

Wang, X., Kang, Q., Shen, D., Zhang, Z., Li; J., Chen, L., 2014. Talanta 124, 7-13.

Weber, J. A., van Zanten, A. P., 1991. Clin. Chem. 37, 695-700.

Wulff, G., 2013. Microchim. Acta 180, 1359-1370.

Wu, L., Ding, F., Yin, W., Ma, J., Wang, B., Nie, A., Han, H., 2017 Anal. Chem. 89, 7578-7585.

Xiao, F., Zeng, Z., Liu, B., 2015. J. Am. Chem. Soc. 137, 10735-10744.

Xie, C., Gao, S., Guo, Q., Xu, K., 2010. Microchim. Acta 169, 145-152.

Yamato, H., Ohwa, M., Wemet, W., 1995. Anal. Chem. 67, 2776-2780.

Yang, B., Li, J., Zhang, L., Xu, G., 2016. Analyst 141, 5822-5828.

Yao, Y., Miao, S., Liu, S., Ping, L., Sun, H., Wang, S., 2012. Chem Eng J. 184, 326-332.

Zhang, X., Tan, X., Zhang, B., Miao, W., Zou, G., 2016. Anal. Chem. 88, 6947-6953.

Zhao, Y., Bi, C., He, X., Chen, L., Zhang, Y., 2015. RSC Adv. 5, 70309-70318.

Zhao, M., Chen, A. Y., Huang, D., Zhuo, Y., Chai, Y. Q., Yuan, R., 2016. Anal. Chem. 88 ,11527-11532.

Fig. 1. (A) HRTEM image and TEM histogram and Gauss fitting of particle size distribution of Ni NCs (inset), (B, C) AFM images of Ni NCs, (D) UV-vis absorption of Ni NCs and PL spectra of Ni NCs with various excitation wavelengths (The inset in part A: photographs of the Ni NCs aqueous solution taken under visible light (lamp off) and 365 nm UV light (lamp on)), (E) The PL and ECL emission spectra of Ni NCs, and (F) FTIR spectra of BSA (a, red line) and Ni NCs@BSA (b, blue line). (G) XRD pattern of Ni NCs, (H) XPS spectra showing the full region of Ni NCs, and (I) Ni 2p region.

Fig. 2. (A, B) SEM images of MIP electrode, (C, D) SEM images of NIP electrode.

Fig. 3. (A) PL responses of the Ni NCs in different concentrations of creatinine, (B) The corresponding relationship between the PL intensity and the logarithm of creatinine concentration, (C) Overlapping spectra for emission of Ni NCs (a) and absorption of creatinine (b), (D) ECL response of MIP-ECL sensor in the absence and presence of creatinine.

Fig.4. (A) ECL responses of the proposed sensor in different concentrations of creatinine in 0.1 M pH 7.4 PBS containing 10 mM TPrA, scanning from 0 V to 1.5 V with a scan rate of 100 mV s^{-1}, (B) The corresponding relationship between the ECL intensity and the logarithm of creatinine concentration. (C) Effects of various interference species on the ECL signal response. (D) The ECL signal response measured by the optimal ECL sensor for MIP and NIP, (E) Effects of various ions on the ECL signal response, (F) The stability of the MIP-ECL developed sensor based Ni NCs/TPrA system under 10 consecutive cyclic potential scans.

Scheme 1. Schematic representation of the MIP-ECL assay for the detection of creatinine.

Table 1A. Comparison the analytical performance of different methods for creatinine detection. (B) recovery study carried out in real samples for creatinine determination by the proposed sensor .

Table 1A. Comparison the analytical performance of different methods for creatinine detection

Detection method	Linear range (μM)	Detection limit (μM)	Reference
Electrochemical	370-3600	8.6	(Chen et al., 2006)
Colorimetric Assay	100-20000	80	(He et al., 2015)
Digital camera based Jaffe reaction	160-1600	89-111	(Debus et al., 2015)
Chemiluminescence	0.1-30	0.007	(Hanif et al., 2016)
MIP-Fluorescent	30-120	25	(Subrahmanyam et al., 2001)
MIP-electrochemical	0.44-17.6	0.35	(Khadro et al., 2010)
MIP-Fluorescent	1-0.1 ×10^6	0.1	This work
MIP-Electrochemiluminesence	0.005 -1000	0.0005	This work

Table 1B. A recovery study carried out in real samples for creatinine determination by the proposed sensor

sample	Measured (μM)	Standard method	Spiked (μM)	Found (μM)	Recovery(%)	RSD(%)
Serum	2.39	2.49	0.5	2.71	93.77	2.26
			5.0	6.85	92.69	2.07
			10.0	12.31	99.51	1.81
Urine	166.90	175.74	5.0	167.2	97.26	2.50
			10.0	170.56	96.41	3.53
			50.0	212.82	98.11	1.91

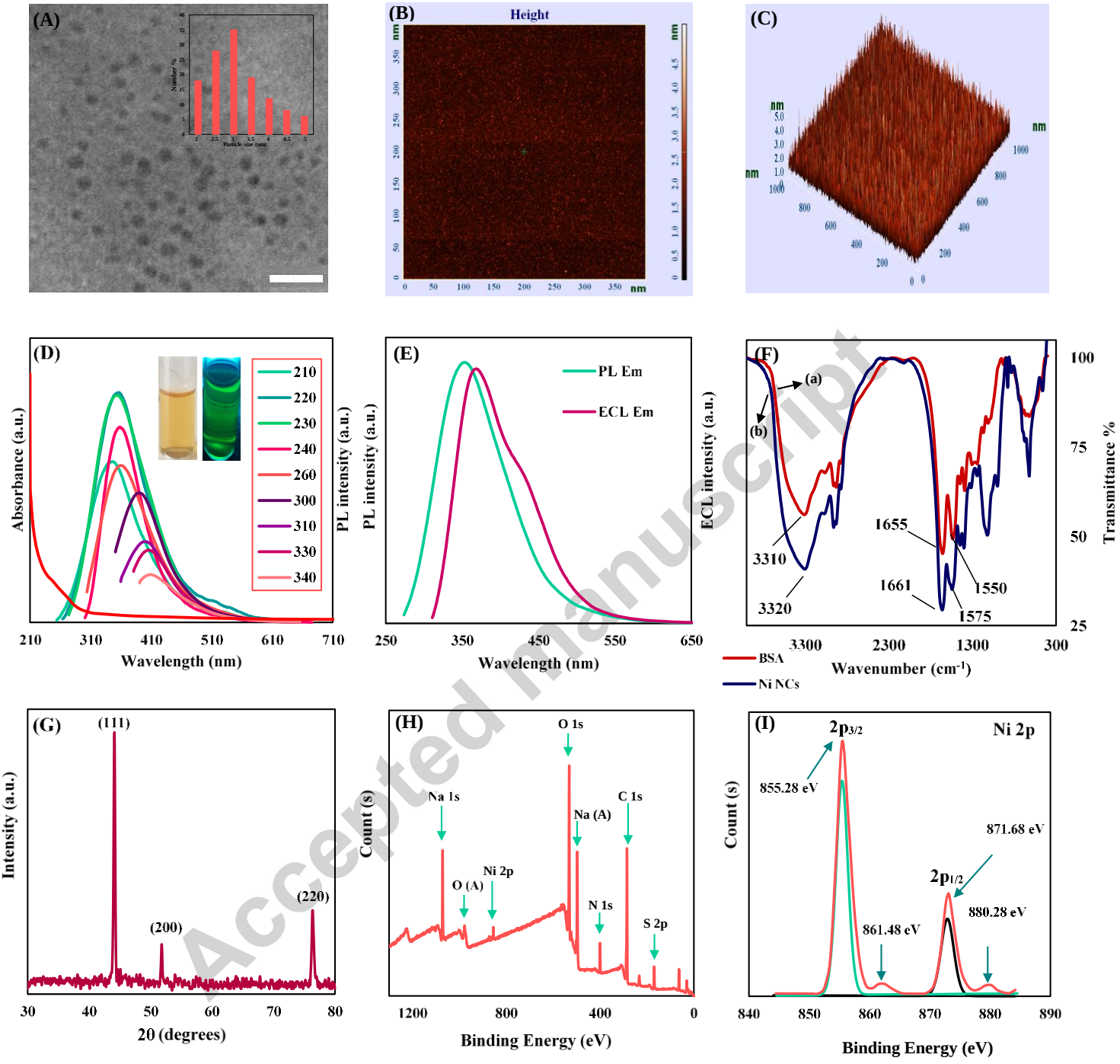

Fig.1

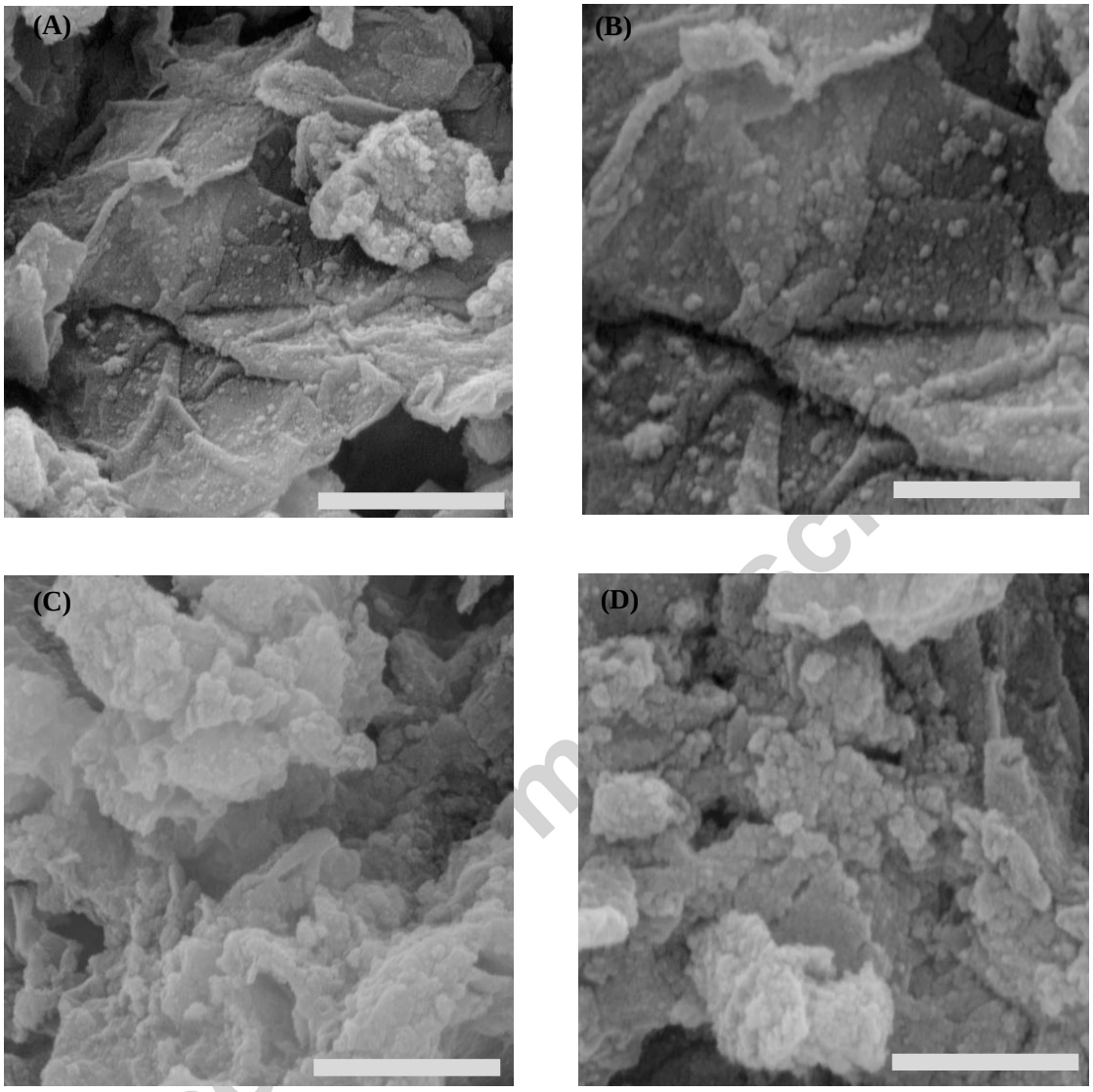

Fig.2

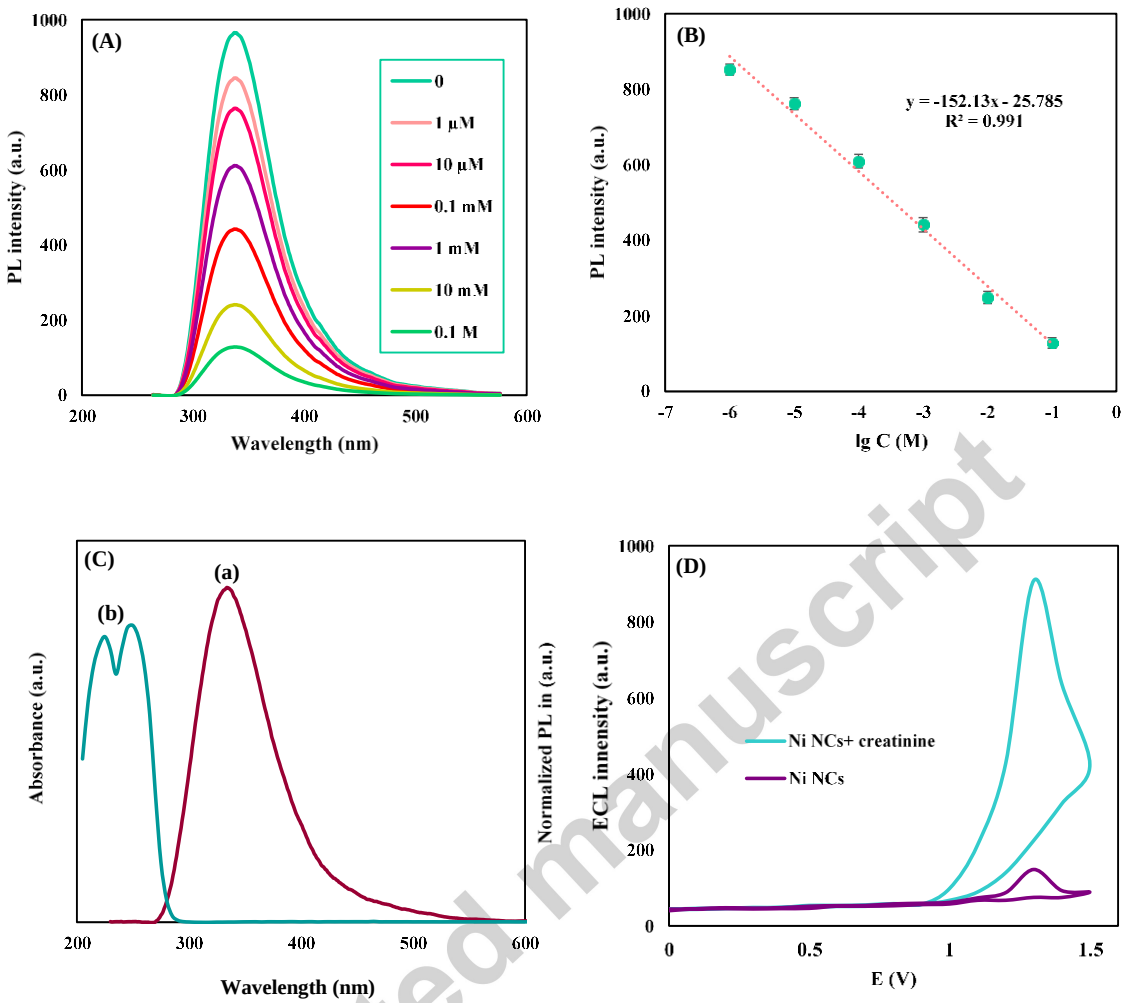

Fig.3

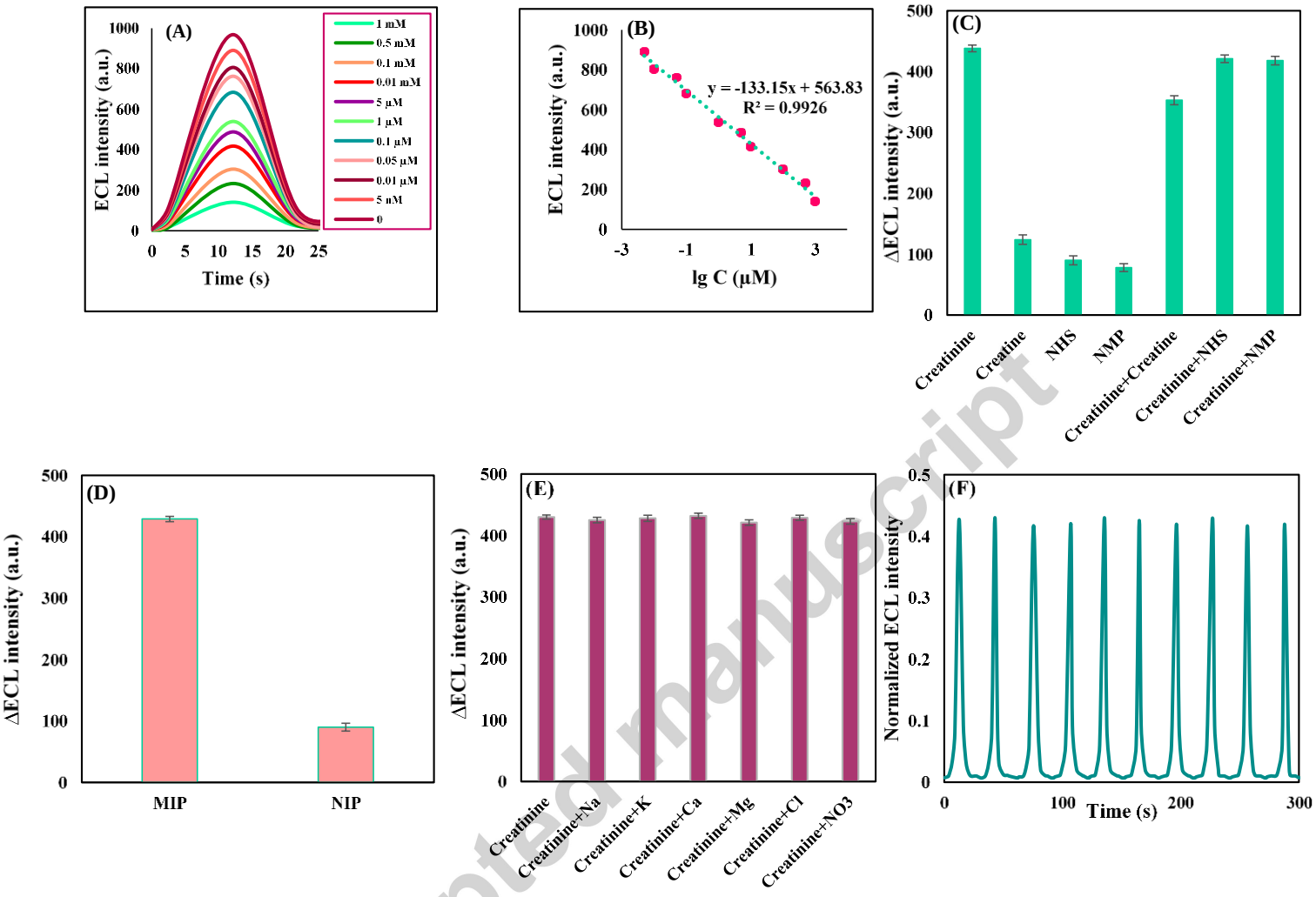

Fig.4

Graphical Abstract

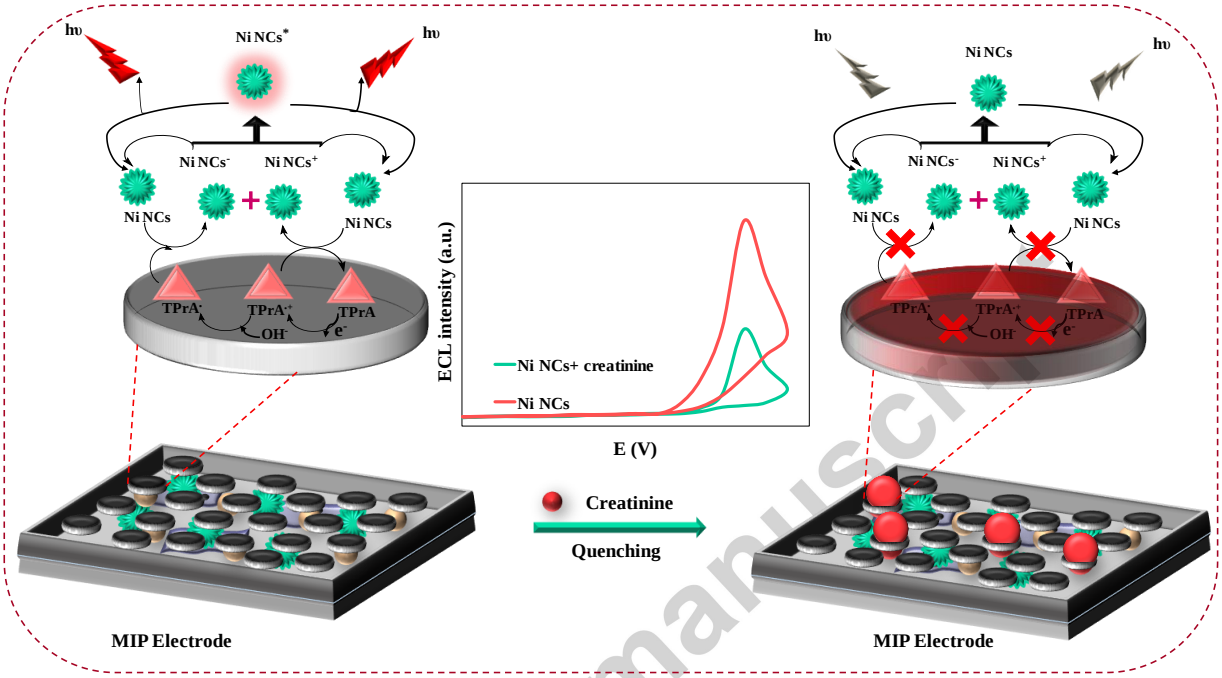

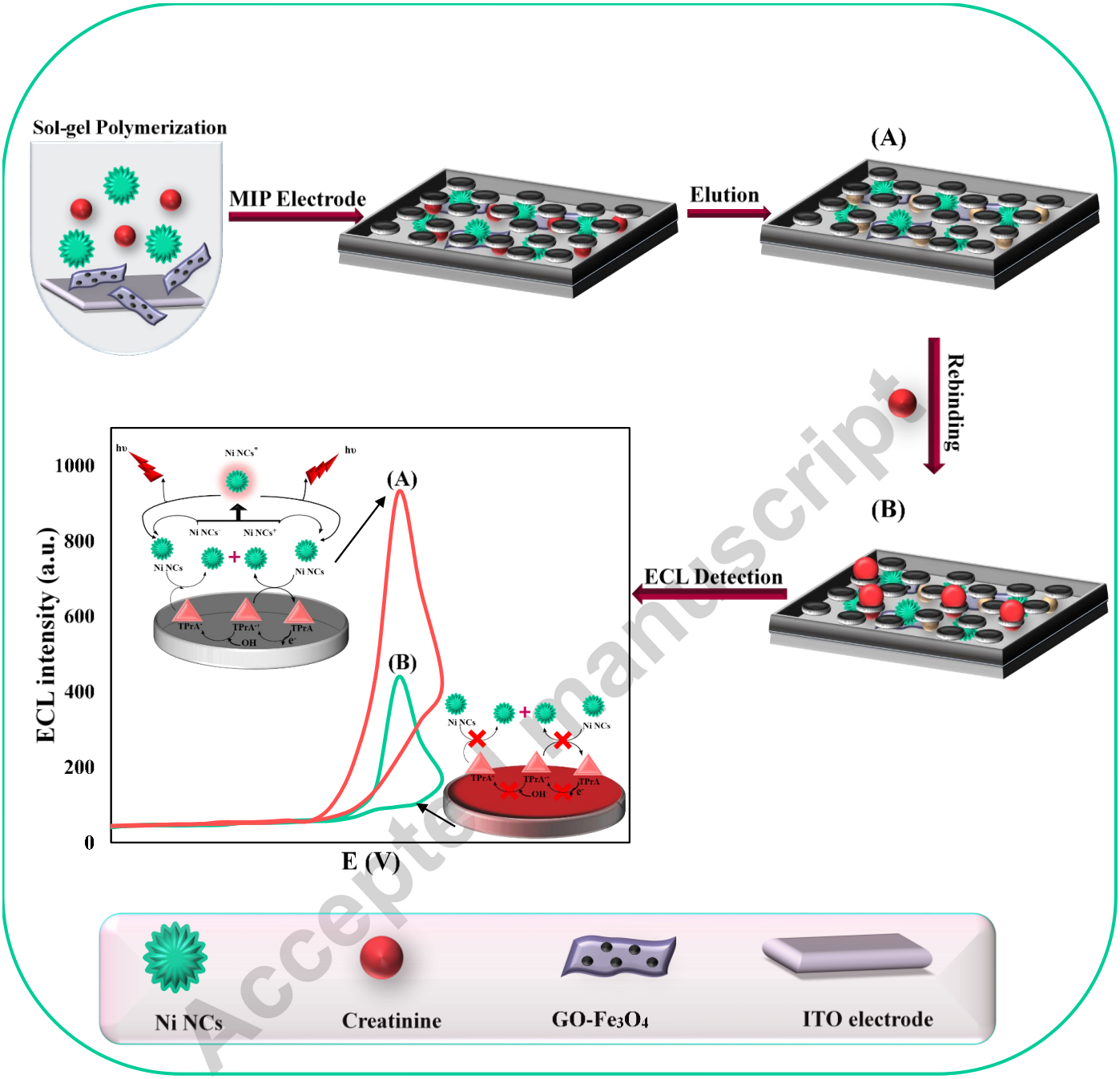

Scheme 1

Highlights

- Ni nanoclusters (NiNCs) used as novel emitter for electrochemiluminescence(ECL) assay.
- ITO electrode modified with MIP/NiNCs used for ECL selective detection of creatinine.

- ECL emission of NiNCs on the MIP-ITO electrode was efficiently quenched by creatinine.
- The ECL-sensor used for nM detection of creatinine in human serum and urine samples.
- NiNCs as novel emitter with MIP improved sensitivity and sensitivity of ECL assays.